HHS Public Access

Author manuscript

Anat Rec (Hoboken). Author manuscript; available in PMC 2016 August 01.

Published in final edited form as:

Anat Rec (Hoboken). 2015 August ; 298(8): 1408–1415. doi:10.1002/ar.23157.

Hyoid bone development: An assessment of optimal CT scanner parameters and 3D volume rendering techniques

Meghan M. Cotter[1,2], **Brian J. Whyms**[1], **Michael P. Kelly**[1], **Benjamin M. Doherty**[1], **Lindell R. Gentry**[3], **Edward T. Bersu**[2], and **Houri K. Vorperian**[1]

[1]Waisman Center, University of Wisconsin-Madison, 1500 Highland Avenue, Madison, WI 53705

[2]Department of Neuroscience, University of Wisconsin-Madison, 1300 University Avenue, Madison, WI, 53706

[3]Department of Radiology, University of Wisconsin Hospital and Clinics, 600 Highland Avenue, Madison, WI 53792

Abstract

The hyoid bone anchors and supports the vocal tract. Its complex shape is best studied in three dimensions, but it is difficult to capture on computed tomography (CT) images and three-dimensional volume renderings. The goal of this study was to determine the optimal CT scanning and rendering parameters to accurately measure the growth and developmental anatomy of the hyoid and to determine whether it is feasible and necessary to use these parameters in the measurement of hyoids from *in vivo* CT scans. Direct linear and volumetric measurements of skeletonized hyoid bone specimens were compared to corresponding CT images to determine the most accurate scanning parameters and three-dimensional rendering techniques. A pilot study was undertaken using *in vivo* scans from a retrospective CT database to determine feasibility of quantifying hyoid growth. Scanning parameters and rendering technique affected accuracy of measurements. Most linear CT measurements were within 10% of direct measurements; however, volume was overestimated when CT scans were acquired with a slice thickness greater than 1.25 mm. Slice-by-slice thresholding of hyoid images decreased volume overestimation. The pilot study revealed that the linear measurements tested correlate with age. A fine-tuned rendering approach applied to small slice thickness CT scans produces the most accurate measurements of hyoid bones. However, linear measurements can be accurately assessed from *in vivo* CT scans at a larger slice thickness. Such findings imply that investigation into the growth and development of the hyoid bone, and the vocal tract as a whole, can now be performed using these techniques.

Keywords

hyoid bone; vocal tract; development; computed tomography (CT)

Corresponding Author: Houri K. Vorperian, Ph.D., Vocal Tract Development Laboratory, Waisman Center, 1500 Highland Avenue, Room 427, Madison, WI 53705, Phone: 608-263-5610, vorperian@waisman.wisc.edu.

INTRODUCTION

The hyoid bone is a small, thin, U-shaped bone that, unlike all other human bones, does not articulate with any other osseous structures. It is the attachment point for nine separate muscles, anchoring the tongue and larynx and playing a vital role in speech production and swallowing (Lieberman et al., 2001). The hyoid bone begins to ossify at the end of the third trimester and may never fully fuse until late in life (Shimizu et al., 2005; Gupta et al., 2008; Sedaghat et al., 2012). The oral and pharyngeal cavities are collectively known as the vocal tract (VT), which is defined as the curvilinear distance from the lips to the glottis. During postnatal growth, there is anatomic restructuring of the human VT, as the oral and pharyngeal structures increase in length and change in shape. As the VT lengthens, the glottis endpoint moves from a position immediately inferior to the oropharynx in infants (at cervical spine level C2–C3) to one that is much lower in adults (cervical spine levels C4–C5). This is due to the descent of both the larynx and the hyoid bone, since the two are structurally connected and functionally related (Fitch and Giedd, 1999). The primary phase of hyo-laryngeal descent occurs before the age of two years, and a smaller secondary descent occurs during puberty in males (Westhorpe, 1987; Fitch and Giedd, 1999; Lieberman et al., 2001; Vorperian et al., 2009; Vorperian et al., 2013).

Many studies have used individual skeletonized hyoid bones to assess sex and age (Papadopoulos et al., 1989; Kim et al., 2006; Mukhopadhyay, 2012). Studies of skeletonized hyoid bones are usually limited to specimens from cadavers of older individuals and thus do not offer a developmental perspective. Analysis of skeletonized hyoid specimens allows for multiple linear and angular measurements of the bones themselves, but reveals nothing about the position of the hyoid bone in relation to other bony structures such as the mandible and the larynx.

Study of the growth and development of the hyoid bone requires *in vivo* visualization, which can be achieved using two-dimensional (2D) lateral cephalograms (Tsai, 2002; Sheng et al., 2009; Phoenix et al., 2011). However, only a few points of the hyoid bone are available for measurement in lateral cephalograms (the hyoidale, the most anterior point of the hyoid bone, being the most common). Two-dimensional imaging of the hyoid bone does not allow for measurement of its width, angle of inclination, volume; or assessment of its degree of ossification.

Three-dimensional (3D) *in vivo* imaging has the combined advantages of skeletonized bone measurement and 2D imaging and permits assessment of hyoid bone shape and dimensions as well as its growth relative to other structures during the course of development. Computed tomography (CT) scans are effective for *in vivo* imaging of osseous structures. Anatomical measurements (such as length, width and volume of bones) taken from CT scans have been verified on larger bones such as femurs, humeri and mandibles (Stull et al., 2013; Whyms et al., 2013). These studies have shown that measurements gathered from CT scans are accurate, but that scanning and reconstruction parameters are complex and must be precise. For example, clear and distinct visualization of the hyoid bone on thick slice (3–5 mm) CT scans can be somewhat difficult due to its small size, shape and degree of ossification. Furthermore, the soft tissue structures that encompass the hyoid bone can

approach a similar density to the hyoid bone and make it difficult to separate on *in vivo* CT scans.

The overall goal of our research is to quantify the typical growth and development of the soft and hard tissue structures of the human vocal tract, specifically the hyomandibular complex. Previous investigations of vocal tract development have tended to assess the vocal tract as a whole rather than assessing its component parts (Abramson et al., 2009; Dalal et al., 2009). While investigations on the development of the entire VT are important, it is equally important to assess the individual parts that provide the skeletal framework within which the various functions are accomplished. The purpose of this study is to determine optimal parameters to scan and model 3D volume rendered images of the hyoid bone to establish a methodology to accurately assess *in vivo* hyoid bone growth and development. Additionally, to determine feasibility of using retrospective imaging studies to quantify growth, we present pilot data of *in vivo* assessment of the growth of the hyoid bone during the first two decades of life using an extant developmental CT imaging database.

MATERIALS AND METHODS

Specimens and subjects

For this study we measured dry bone hyoid specimens directly and also made *in vivo* measurements of a select subset of the hyoid bones using their CT scans. Five dry hyoid bones were obtained from the Department of Neuroscience (source I) and the Department of Anthropology (source II) at the University of Wisconsin-Madison. The two completely ossified hyoid bones (one adult and one child; from source I) had previously been used as teaching specimens, and exact ages could not be determined. The three unfused hyoid bones (from source II) had related os coxae bones, and age ranges were estimated from the pubic symphysis (Table 1). Lastly, an acrylic prism (polymethyl 2-methylpropenoate) of known size and volume was used as a control for comparison (Whyms et al., 2013).

The Vocal Tract Development Laboratory curates a large retrospective database of head and neck CT scans performed at the University of Wisconsin Hospital and Clinics (UWHC). The imaging database was developed over the past decade, with approval from University of Wisconsin Health Sciences Institutional Review Board, for the purpose of assessing the growth and development of head and neck structures that serve the functions of respiration, food ingestion and deglutition, and speech production. For this pilot investigation, twenty cases (10 male, 10 female) were selected to represent different ages during the first two decades of life to assess growth of the hyoid bone and to investigate the feasibility of using standard retrospective images to investigate said growth.

Procedures

Computed tomography scanning—The fused adult hyoid bone and fused child hyoid bone from source I and the prism were scanned at UWHC using a General Electric LightSpeed 16 MSCT scanner (General Electric Medical Systems, Milwaukee, WI) (Fig. 1). The hyoid bones were enclosed in plastic wrap and submerged in water inside a plastic container to reduce the effects of beam hardening. The hyoid bones and prism were each

scanned with CT acquisition parameters of 14.0 cm FOV, 100.0 mÅ, 80 kV. All hyoid bones were scanned with slice thicknesses of 0.625 mm, 1.25 mm and 2.50 mm. The images were reconstructed using both General Electric standard and bone-plus algorithms.

All of the *in vivo* head and neck scans from the retrospective imaging database had been taken at the UWHC and anonymized in compliance with UW Health Sciences Institutional Review Board standards and guidelines. All scans were acquired using 2.5 mm slice thickness images using a 14.0–20.0 cm FOV, 170.0–300.0 mÅ, 120–140 kV, and were reconstructed with both standard and bone-plus algorithms.

Measurement accuracy: Linear and volume measurement of specimens—To assess the accuracy of measurements taken from CT scans, linear and volumetric measurements taken directly from the dry specimens were compared to equivalent measurements taken from their 2.5 mm slice thickness 3D segmented models using Analyze 10.0 (AnalyzeDirect, Overland Park, KS, USA). Linear measurements of the dry hyoid bones and the prism were taken using digital calipers (KURT Precision Instruments, Minneapolis, MN, Model EC6). Five linear measurements were taken: a) hyoid body depth, b) greater cornu length-left, c) total length, left, d) greater cornu width and e) total length of hyoid left (see Table 1 and Figure 1). The prism's x, y and z landmarks were its clearly defined edges, corners and planes.

Due to the small size and low density of the hyoid bones, it was not possible to use conventional means of obtaining volume directly (i.e., water displacement). Instead, the suspension technique, a variation on hydrostatic weighing, was used (Hughes, 2005). The hyoid specimens were each enclosed in a single layer of plastic wrap, weighted with a small sinker and suspended in a beaker full of water that was placed on a digital scale (Fisher Scientific Accu-2202). The volume of the hyoid specimen was obtained using Archimedes' principle:

$$V = \Delta w / \rho \quad \text{(Eq. 1)}$$

Where V equals the volume of each hyoid specimen (cm^3), Δw is the change in weight (g) recorded by the scale when the hyoid specimen was suspended in the water (minus the suspended weight of the sinker) and ρ is the density of water at 70 °F (g/cm^3). The volume of each hyoid specimen was measured three times and the results were averaged. Similarly, the volume of the prism was determined by both water displacement and suspension and compared for verification.

Segmentation and landmarking of specimens—Analyze 10.0 software (AnalyzeDirect Inc., Overland Park, KS, USA) was used to open the DICOM CT scan files of the dry hyoid specimens and prism and to visualize and render 3D models. The 3D hyoid specimen models were constructed from the standard algorithm using two different segmentation methods: global threshold segmentation and region-specific threshold segmentation (using the Volume Edit tool in Analyze). In the global threshold method, a single threshold was applied to all the images of each specimen and then adjusted by visual inspection using the Region of Interest tool in Analyze to find the most appropriate

threshold for segmentation. A region specific method of thresholding could account for changes in density throughout the hyoid bone. In the region-specific threshold method, the hyoid models were generated slice-by-slice using the Volume Edit tool in Analyze, where the threshold was adjusted by visual inspection on a per slice basis and recorded. Since the above methods require manual inspection, we additionally reconstructed the 3D models using a fully automated thresholding technique, half-maximum height (Coleman and Colbert, 2007; Weber and Bookstein, 2011), on both a global and per-slice scale. However, this technique was unable to model the small, variable density hyoid bone with sufficient accuracy. Large portions of the bone were excluded when using both global and per-slice HMH techniques. Therefore the analyses in the remainder of this study utilize data collected using the visually inspected threshold method.

Next, the fabricate tool in Analyze was used to place landmarks on the 3D hyoid bone models to make linear measurements. Multiplanar orthogonal sections of the CT scan were used to ensure accurate landmark placement on the 3D models. The x, y and z coordinates of the landmark were recorded within the CT scan. The coordinates of the landmarks were then used to calculate the distances between the landmarks that corresponded to the linear measurements taken on the dry specimens (hyoid body width, left greater cornu length and total length of hyoid bone). Volume of the hyoid bone models and prism was measured using the Volume Render tool.

To determine the most accurate method of reconstructing hyoid bones from *in vivo* head and neck scans, the *in vivo* hyoid bones from the imaging database were thresholded using both the global threshold method and the region-specific threshold method. In addition, global threshold levels assigned to the adjacent mandible in a previous study (Whyms et al. 2013) were used. Threshold ranges (in Hounsfield Units, HU) were recorded and compared between each method and with age of each case. Next, linear measurements of the *in vivo* hyoid bone scans that corresponded with the dry bone analyses were collected as pilot data to compare the change in hyoid bone growth with age.

Statistical analysis—Direct linear and volume measurements of hyoid bone specimens and the prism were compared to CT linear and volume measurements using percent error:

$$\{(\text{CT value} - \text{direct value})/\text{direct value}\} \times 100. \quad \text{(Eq. 2)}$$

Paired t-tests were used to compare the volume of the *in vivo* hyoid bones between the global threshold and the region-specific threshold methods. Global thresholds from the current study were compared to the global thresholds from the mandible study using paired t-tests. The *in vivo* CT scan linear measurements were also plotted versus age as pilot data to assess growth over time. R-squared values of regression models were used to determine the best fit to the data. All statistical analyses were completed using SPSS 20.

RESULTS

Linear and volume measurement of specimens

Linear measurements collected from the CT scans of the hyoid specimens varied in their accuracy when compared to direct measurements (Table 2). Linear measurements from the models created using the region-specific thresholding method were all within 10% error except Hyoid Body Depth (see Discussion).

The measured 3D CT volumes of the fused hyoid bones (Hyoid bones 1 and 2) were inversely related to acquisition slice thickness, i.e., the thinnest slices (0.625 mm) had the lowest volume and the thickest slices (2.5 mm) had the highest volume (See Table 3). Compared to direct measurements, the CT scan at 0.625 mm slice thickness yielded the most accurate volume for Hyoid bone 1 and a slice thickness of 1.25 mm yielded the most accurate volume for Hyoid bone 2. The measured prism 3D volume was also slice thickness-dependent, and the thinnest slices (0.625 mm) yielded the most accurate prism volume.

The slice thickness of 2.5 mm (the most common resolution used in head and neck CT scans) greatly overestimated the volumes of both the adult and child hyoid specimens (percent error: 19–91%) (Table 3). Table 3 also shows that, as expected, the unfused adult hyoid specimens (Hyoid bones 3, 4 and 5) had lower volumes than the fused adult hyoid specimen (Hyoid bone 2). All of the adult hyoid specimens had higher volumes than the child hyoid specimen (Hyoid bone 1).

In vivo hyoid data

Threshold comparison—Global thresholding of the *in vivo* hyoid bones used a smaller range of threshold levels (105–170 HU) than the region-specific method (85–354 HU), as well as lower mean, median and mode of the threshold levels used in modeling (Table 4). There was no correlation between mean threshold and volume ($R^2 = 0.08$, $p = 0.22$); however there was a correlation between mean threshold and age ($R^2 = 0.44$, $p < 0.001$). Higher thresholds were used when segmenting the images from older individuals.

As seen in Figure 2, it is evident that using the same threshold as the adjacent mandible would be problematic, since portions of the greater cornu of the hyoid bone completely disappear on 3D models at mandible threshold levels. T-tests between thresholds of adjacent mandible and hyoid bones rendered using a global threshold in *in vivo* studies revealed that the threshold levels were significantly different ($p = 0.04$). Importantly, when the mandibular threshold was applied to the hyoid bones, the volumes of the hyoid bones were significantly lower than if the mandible and hyoid bones were thresholded separately ($p < 0.001$). These data indicate that threshold levels for the mandible and hyoid bone should be chosen separately to maintain accurate 3D volume measurements.

Hyoid growth pilot data—Figure 3 displays a sample of developmental pilot data collected using *in vivo* scans during the first two decades of life. All measurements showed a rapid period of growth during the first few years of life, with discrete differences in growth of different portions of the hyoid bone after about age 6–8 years (Fig. 3). The sensitivity of the data to capture developmental changes is also apparent with sex-specific differences in

the growth pattern of greater cornu width between males and females that is apparent after 150 months (12.5 years), coinciding with the expected onset of puberty.

DISCUSSION

The overall goal of our research is to understand the growth and development of the human vocal tract as it carries out its functions of fluid and food ingestion, respiration, and vocalization/speech production. A detailed understanding of the growth and development of the hyoid bone is warranted given the important functions it serves and the fact that there is hardly any information available on its three-dimensional growth. The purpose of this study was to determine optimal CT image acquisition parameters for accurately visualizing and measuring the hyoid bone and to assess the feasibility and necessity of using such measures to quantify its growth using *in vivo* medical imaging studies, specifically CT studies. An important contribution of this study was determining the accuracy of 2D and 3D CT measurements of dry, skeletonized hyoid bones when compared to similar "gold-standard" *ex vivo* measurement. This direct comparison allows for verification of 2D and 3D measurement accuracy on CT scans. Limitations of the study include a small sample size and unknown age of the fused hyoid specimens. Despite these limitations, however, the methodology confirms the feasibility of implementing large scale studies using *ex vivo* skeletonized hyoid bones and *in vivo* hyoid bones segmented from retrospective CT scans to assess hyoid bone growth and development.

Comparison of measurements of dry, skeletonized hyoid bones with CT images of these same bones revealed that thinner CT slices (i.e., slice thickness of 1.25 mm or less) yielded the most accurate 3D models. The most common slice thickness used in clinical protocols for this region is around 2.5 mm. Therefore, if the volume of the hyoid bone is to be assessed from CT scans utilizing a 2.5 mm slice thickness, it is necessary to understand that volumetric measurements of the hyoid bone will be inflated. Furthermore, volumetric assessments should be used only to approximate the general growth trend of the hyoid bone, not its actual volume during growth. Nevertheless, most of the linear measurements were within a 10% error above the actual measurement. Since volume was overestimated for the hyoids, slight overestimation of linear measurements is to be expected. As noted in Table 2, the measurements of the adult dry bone hyoid (Hyoid 2) were more accurate than the child hyoid (Hyoid 1). The larger overall size of Hyoid 2 likely influenced this difference. It is possible that finer resolution would reduce the error of the linear measurements, but this would also limit the number of usable retrospective scans from our cohort to examine the developmental growth trend of the hyoid bone. This is due to the clinical prevalence of using 2.5mm resolution over thinner slices to minimize exposure to radiation. Thus, given the benefits of a larger sample size particularly for a developmental study, we deemed this percent error as acceptable for a CT scan slice thickness of 2.5mm.

Threshold method also affects measurement accuracy. Three-dimensional images of hyoid bones reconstructed using the region-specific method yielded linear measurements that were more accurate than those using the global threshold method. The region-specific method also allowed for better visualization of the hyoid cornu than the global threshold method. Optimal global thresholds for 3D reconstructions of the mandible were not optimal for the

hyoid bones and caused portions of the cornu to be variably excluded from the 3D model. These 3D images were deemed totally unacceptable for making linear measurements (Fig. 2). We therefore do not recommend using composite global thresholding using the same threshold for all skeletal elements in a single CT scan. Variable thickness of the skeletal elements and density of the tissues in the head and neck region require a more fine-tuned approach when creating 3D models, and the region-specific method proved to be the most accurate.

Preliminary data from 3D modeling of *in vivo* hyoid bone scans indicate that threshold levels were not significantly related to measured 3D volume. These data did indicate, however that older individuals required higher thresholds. This is likely due to increased size and density of the hyoid bone over time. Furthermore, pilot data revealed that although the growth trend of the different component parts of the hyoid bone were similar during the first few years of life, some measurements increased more than other measurements. There appears to be a divergence in growth trend where some measurements continue to grow at the same rate (e.g., total hyoid length, Fig. 3D), others show a decline in growth rate (e.g., total length, Fig. 3B), while other structures seem to have a second phase of rapid growth during puberty (e.g., cornu length, Fig. 3A). Additional investigations for a thorough assessment of hyoid growth are, therefore, warranted, particularly during periods where rapid growth is expected such as during the first few years of life and during puberty. Analysis beyond the first two decades of life is also warranted given documentation on the fusion of the hyoid body with the cornu (Shimizu et al., 2005; Gupta et al., 2008; Sedaghat et al., 2012).

The advent of 3D CT modeling and measurement techniques allows for investigations using non-traditional measurements. For example, further investigation on greater cornu width is warranted given the apparent sexual dimorphism in its growth pattern (Fig. 3). This is a novel measurement because classically the vocal tract has been assessed in the sagittal plane with focus on anteroposterior measurements. Further investigation of three-dimensional changes of the hyoid bone and of its relationship to other vocal tract structures (mandible, tongue, larynx, etc.) will permit a more thorough understanding of differences between males and females during childhood and adolescence.

Understanding growth and development of anatomical structures using non-destructive techniques such as 3D CT scans is still a relatively new endeavor. Given that risk of ill effects from radiation on the developing head and neck of children, prospective growth studies are not practical. It will be important to develop and utilize the most proper techniques to gather data from retrospective studies. This will allow the ability to optimize measurements on newly acquired scans and will provide a venue to salvage heretofore unused developmental data from large scale collections of existing CT scans.

Acknowledgments

This work described in this paper was supported by NIH Grant R01 DC006282 from the National Institute on Deafness and Other Communicative Disorders (NIDCD), also P-30 HD0335 from the National Institute of Child Health and Human Development (NICHD). The authors thank Dr. John Hawks of the Department of Anthropology at the University of Wisconsin-Madison for his generosity in providing hyoid bone specimens for analysis. The authors also thank Diana Drier of Waisman Center Biomanufacturing for facilitating the use of scales and lab

equipment for weighing the hyoid bones for volumetric assessment; Ellie Fisher and Simon Lank for help with preparation of figures; and Drs. Sean Fain and Chihwa Song, for guidance with methodology verification.

LITERATURE CITED

Abramson Z, Susarla S, Troulis M, Kaban L. Age-related changes of the upper airway assessed by 3-dimensional computed tomography. J Craniofac Surg. 2009; 20(Suppl 1):657–663. [PubMed: 19182684]

Coleman MN, Colbert MW. Technical note: CT thresholding protocols for taking measurements on three-dimensional models. Am J Phys Anthropol. 2007; 133:723–725. [PubMed: 17326102]

Dalal PG, Murray D, Messner AH, Feng A, McAllister J, Molter D. Pediatric laryngeal dimensions: an age-based analysis. Anesth Analg. 2009; 108:1475–1479. [PubMed: 19372324]

Fitch WT, Giedd J. Morphology and development of the human vocal tract: A study using magnetic resonance imaging. J Acoust Soc Am. 1999; 106:1511–1522. [PubMed: 10489707]

Gupta A, Kohli A, Aggarwal NK, Banerjee KK. Study of age of fusion of hyoid bone. Leg Med (Tokyo). 2008; 10:253–256. [PubMed: 18442944]

Hughes S. Archimedes revisted: a faster, better, cheaper method of accurately measuring the volume of small objects. PHysics Education. 2005; 40:468–474.

Kim DI, Lee UY, Park DK, Kim YS, Han KH, Kim KH, Han SH. Morphometrics of the hyoid bone for human sex determination from digital photographs. J Forensic Sci. 2006; 51:979–984. [PubMed: 17018072]

Lieberman DE, McCarthy RC, Hiiemae KM, Palmer JB. Ontogeny of postnatal hyoid and larynx descent in humans. Arch Oral Biol. 2001; 46:117–128. [PubMed: 11163319]

Mukhopadhyay PP. Determination of sex from an autopsy sample of adult hyoid bones. Med Sci Law. 2012

Papadopoulos N, Lykaki-Anastopoulou G, Alvanidou E. The shape and size of the human hyoid bone and a proposal for an alternative classification. J Anat. 1989; 163:249–260. [PubMed: 2606777]

Phoenix A, Valiathan M, Nelson S, Strohl KP, Hans M. Changes in hyoid bone position following rapid maxillary expansion in adolescents. Angle Orthod. 2011; 81:632–638. [PubMed: 21306225]

Sedaghat AR, Flax-Goldenberg RB, Gayler BW, Capone GT, Ishman SL. A case-control comparison of lingual tonsillar size in children with and without Down syndrome. Laryngoscope. 2012; 122:1165–1169. [PubMed: 22374875]

Sheng CM, Lin LH, Su Y, Tsai HH. Developmental changes in pharyngeal airway depth and hyoid bone position from childhood to young adulthood. Angle Orthod. 2009; 79:484–490. [PubMed: 19413400]

Shimizu Y, Kanetaka H, Kim YH, Okayama K, Kano M, Kikuchi M. Age-related morphological changes in the human hyoid bone. Cells Tissues Organs. 2005; 180:185–192. [PubMed: 16260865]

Stull KE, L'abbé EN, Steiner S. Measuring distortion of skeletal elements in Lodox Statscan-generated images. Clin Anat. 2013; 26:780–786. [PubMed: 23362110]

Tsai HH. The positional changes of hyoid bone in children. J Clin Pediatr Dent. 2002; 27:29–34. [PubMed: 12413169]

Vorperian HK, Wang S, Chung MK, Schimek EM, Durtschi RB, Kent RD, Ziegert AJ, Gentry LR. Anatomic development of the oral and pharyngeal portions of the vocal tract: an imaging study. J Acoust Soc Am. 2009; 125:1666–1678. [PubMed: 19275324]

Vorperian, HK.; Wang, Y.; Durtschi, RB.; Cotter, MM.; Kent, RD.; Chung, MK.; Gentry, LR. Anatomic development of the hyo-laryngeal complex in humand from birth to 95 years: an imaging study. Acoustical Society of America; San Francisco, CA: 2013.

Weber, GW.; Bookstein, FL. Virtual Anthropology: A guide to a new interdisciplinary field. New York: Springer; 2011.

Westhorpe RN. The position of the larynx in children and its relationship to the ease of intubation. Anaesth Intensive Care. 1987; 15:384–388. [PubMed: 3425879]

Whyms BJ, Vorperian HK, Gentry LR, Schimek EM, Bersu ET, Chung MK. The effect of computed tomographic scanner parameters and 3-dimensional volume rendering techniques on the accuracy

of linear, angular, and volumetric measurements of the mandible. Oral Surg Oral Med Oral Pathol Oral Radiol. 2013; 115:682–691. [PubMed: 23601224]

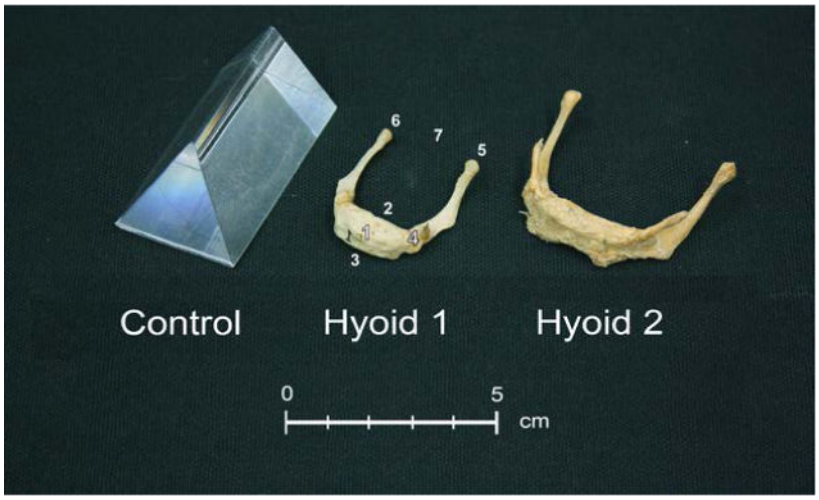

Figure 1.

Specimens scanned: Prism, Hyoid 1 (child) and Hyoid 2 (adult). Hyoid 1 is labeled to reflect anatomic landmarks listed in Table 1: (1) hyoidale, (2) hyoid body posterior superior, (3) hyoid body anterior inferior, (4) greater cornu base left, (5) greater cornu apex left, (6) greater cornu apex right, and (7) greater cornu width midpoint.

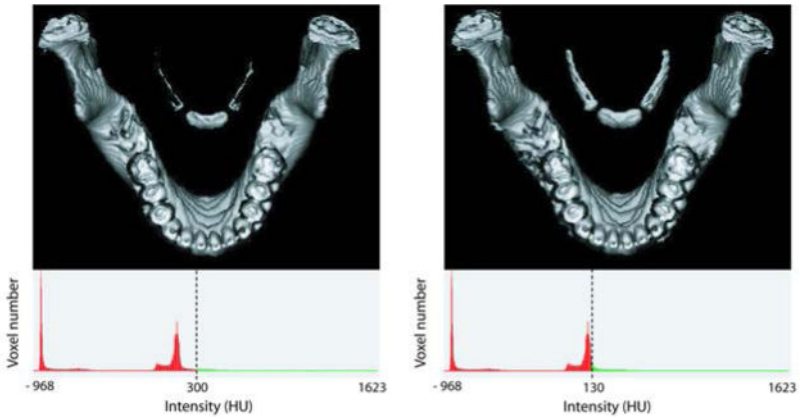

Figure 2.

Hyoid-mandible pairs segmented with different HU thresholds: standard bone (global) threshold (left) and hyoid-specific threshold (right). The hyoid bone has a lower Hounsfield CT density than the mandible on CT. The typical threshold parameters for bone of the mandible, excludes significant portions of the hyoid bone, particularly the cornua (left image). The hyoid-specific threshold depends on structure size/age.

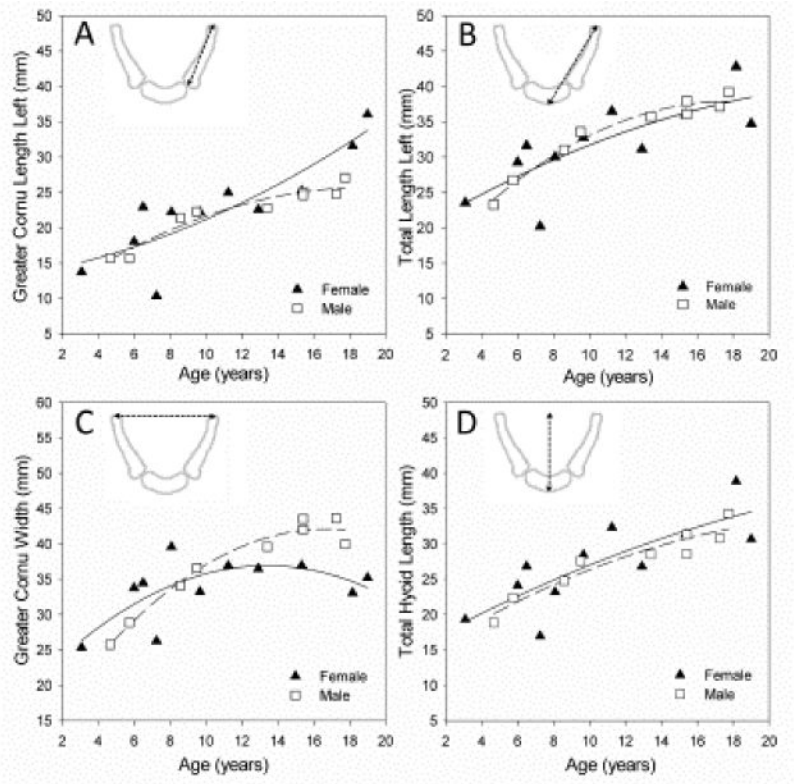

Figure 3.

Developmental growth pilot data, ages 2 – 20, from *in vivo* CT scans. Hyoid landmarks were placed, and linear measurements taken as described in Table 1. Figure 3 displays the feasibility of using the segmentation and analysis methods presented to quantify growth using retrospective imaging studies. Despite variability in the growth trend of the different measurements, all variables show a rapid period of growth during the first few years of life with discrete differences in growth after about age 6–8 years, as well as male/females differences in growth.

Table 1

Hyoid landmarks and linear measurements defined (see Fig. 1).

#	Landmark	Abbreviation	Description
1.	Hyoidale	Hy	The most superior and anterior point in the sagittal midline of the hyoid body.
2.	Hyoid Body Posterior Superior	Hps	The most posterior and superior point in the sagittal midline of the hyoid body.
3.	Hyoid Body Anterior Inferior	Hai	The most inferior point in the sagittal midline of the hyoid body.
4.	Greater Cornu Base Left	GrCorBL	The base or most proximal point of left greater cornu (in individuals with fused hyoid bones, the midpoint of joint between body and cornu on anterior surface).
5.	Greater Cornu Apex Left	GrCorAL	The apex or most superior and distal endpoint of the left greater cornu.
6.	Greater Cornu Apex Right	GrCorAR	The apex or most superior and distal endpoint of the right greater cornu.
7.	Greater Cornu Width Midpoint	GrCorWM	The midpoint of the line extending from the apex of the left greater cornu to the apex of the right greater cornu (calculated using all three dimensions in Analyze 10.0).
	Linear Measurement	Landmarks	Description
2–3	Hyoid Body Depth	Hps-Hai	In the sagittal plane, distance from the most posterior and superior point of the hyoid body to the most inferior point of hyoid body.
5–4	Greater Cornu Length Left	GrCorAL-GrCorBL-	Distance from the apex (most superior and distal endpoint) of left greater cornu to the base (most proximal point) of left greater cornu.
5–1	Total Length Left	GrCorAL-Hy-	Distance from the apex of the left greater cornu to the most superior and anterior point of the hyoid body.
5–6	Greater Cornu Width	GrCorAL-GrCorAR	Distance from the apex of left greater cornu to the apex of right greater cornu.
1–7	Total Hyoid Length Left	Hy-GrCorWM	Distance from the most superior and anterior point in the sagittal midline of hyoid body to the midpoint of the line connecting the apex of the left greater cornu to the apex of the right greater cornu.

Table 2

Comparison of direct and 2.5 mm in-plane resolution CT scan measurements of the child (Hyoid 1) and adult (Hyoid 2) dry bone hyoids.

[1]< 10% error [2]< 5% error	Threshold Type	Volume (cm^3)	Hyoid Body Depth (mm)	Greater Cornu Length Left (mm)	Total Hyoid Length Left (mm)	Greater Cornu Width (mm)	Total Hyoid Length (mm)
Hyoid 1	Direct	1.37	10.60	29.84	38.39	26.60	37.14
	Global	2.62	14.64	33.66	44.72	29.13[1]	42.93
	Region	2.10	12.52	32.74[1]	41.39[1]	28.73[1]	39.68[1]
Hyoid 2	Direct	2.61	10.61	34.10	42.93	45.74	40.82
	Global	3.11	16.80	34.84[2]	47.39	45.73[2]	43.02[1]
	Region	3.18	13.61	35.55[2]	46.84[1]	45.49[2]	43.05[1]

Table 3

Skeletonized hyoid bone specimens and prism volume comparisons. Value in parentheses denotes the difference between CT volume and water suspension volume.

ID	Source	Fused/unfused	Age Range (years)	Sex	Water Suspension Volume (cm^3)	CT Volume (cm^3)		
						Slice Thickness		
						0.625 mm	1.25 mm	2.5 mm
Hyoid 1	I	Fused	<18	Unknown	1.37	1.22 (−0.15)	2.24 (.87)	2.62 (1.25)
Hyoid 2	I	Fused	>18	Unknown	2.61	2.28 (−.33)	2.65 (.04)	3.11 (0.5)
Hyoid 3	II	Unfused	40–50	Male	1.62			
Hyoid 4	II	Unfused	50–60	Female	2.11			
Hyoid 5	II	Unfused	25–30	Male	2.49			
Prism					29.62	29.97 (.32)	30.13 (.51)	30.40 (.78)

Anat Rec (Hoboken). Author manuscript; available in PMC 2016 August 01.

Table 4

Comparison of minimum threshold ranges between global thresholding and region-specific thresholding methods

	Global	Region
Minimum (HU)	105	85
Maximum (HU)	170	354
Mean (HU)	131.10	173.87
Median (HU)	129	175
Mode (HU)	120	146
Quartile1 (HU)	120	146
Quartile3 (HU)	139.75	192